Surface Science 625 (2014) 57–63

Contents lists available at ScienceDirect

Surface Science

journal homepage: www.elsevier.com/locate/susc

Structure of the Co/Si(111) $\sqrt{13} \times \sqrt{13}$ surface revisited

D.A. Olyanich [a,b], T.V. Utas [a], A.A. Alekseev [a], V.G. Kotlyar [a,b], A.V. Zotov [a,b,c], A.A. Saranin [a,b,*]

[a] Institute of Automation and Control Processes, 5 Radio Street, 690041 Vladivostok, Russia
[b] School of Natural Sciences, Far Eastern Federal University, 690950 Vladivostok, Russia
[c] Department of Electronics, Vladivostok State University of Economics and Service, 690600 Vladivostok, Russia

ARTICLE INFO

Article history:
Received 30 January 2014
Accepted 11 March 2014
Available online 17 March 2014

Keywords:
Atom–solid interactions
Silicon
Cobalt
Self-assembly
Scanning tunneling microscopy

ABSTRACT

The Si(111) $\sqrt{13} \times \sqrt{13}$–$R$ 13.9°-Co surface reconstruction shows up in the scanning tunneling microscopy images as an array of clusters. Two types of clusters coexist appearing as dark and bright in the images. P. Wetzel with co-workers (Surf. Sci. 604 (2010) 513 and Surf. Sci. 607 (2013) 111) have recently proposed a structural model of the dark cluster containing three Co atoms located in substitutional sites of the Si(111) surface with overlying triangle of six Si adatoms. The bright clusters have been suggested to contain three additional Si atoms on top of the six Si atoms terminating the dark cluster. The proposed models assume that the Si(111) $\sqrt{13} \times \sqrt{13}$–$R$ 13.9°-Co surface contains 3/13–0.23 ML Co. Our thorough experimental evaluations of the surface composition confirm that the bright cluster adopts three additional Si atoms but unambiguously demonstrate that the actual Co coverage at the Si(111) $\sqrt{13} \times \sqrt{13}$–$R$ 13.9°-Co surface is 1.4 ± 0.2 ML. To reconcile the reported structural models with the newly determined Co coverage, we suggest that the clusters reside not at the bare Si(111) surface (as suggested previously), but on the silicide Si–Co–Si triple layer on Si(111) substrate. Among about forty models with various types of completed and uncompleted silicide interfaces, the two models (with A8- and B8-type interfaces) have been proven to represent the most stable configurations.

© 2014 Elsevier B.V. All rights reserved.

1. Introduction

The last years have been marked to the renewed interest to the initial stages of the interface formation in the Co/Si(111) system [1–6]. A set of the Co-induced Si(111) surface reconstructions has been found, including the so-called "1 ± 1"-RC (ring cluster) structure and ordered $\sqrt{7} \times \sqrt{7}$–R 19.1°, $\sqrt{19} \times \sqrt{19}$–$R$ 23.4° and $\sqrt{13} \times \sqrt{13}$–$R$ 13.9° phases. The "1 × 1" and $\sqrt{7} \times \sqrt{7}$–R 19.1° surfaces have been established to be built of the same structural elements, ring clusters, each composed of a single Co atom in a substitutional silicon position under a six Si adatoms ring [3,5,7,8]. The difference between the two surfaces is that the "1 × 1" phase appears as a random incomplete RC array containing 0.05 to 0.1 ML Co, while the $\sqrt{7} \times \sqrt{7}$–R 19.1° phase is an ordered close-packed hexagonal array of RCs with 1/7 (~0.14) ML Co coverage. [1 ML (monolayer) = 7.8×10^{14} cm^{-2}, the topmost Si atom density at the unreconstructed Si(111)1 × 1 surface]. The $\sqrt{19} \times \sqrt{19}$–$R$ 23.4° reconstruction presents typically as limited-size domains coexisting with other reconstructions, $\sqrt{7} \times \sqrt{7}$–R 19.1° and $\sqrt{13} \times \sqrt{13}$–$R$13.9° [1]. In the scanning tunneling microscopy (STM) images, it looks akin the $\sqrt{19} \times \sqrt{19}$–$R$ 23.4° reconstruction observed in Ni/Si(111) system and has plausibly a similar atomic arrangement, namely, built of the ring clusters consisting of three metal atoms (Ni or Co) in the substitutional Si positions capped by six Si adatoms forming three dimers [9]. Thus, an ideal Co coverage in the $\sqrt{19} \times \sqrt{19}$–$R$ 23.4° phase is 3/19 (~0.16) ML. The next more dense Co/Si(111) reconstruction is the $\sqrt{13} \times \sqrt{13}$–$R$ 13.9° [2,4,6,10]. Remarkably, formation of a $\sqrt{13} \times \sqrt{13}$–$R$ 13.9° reconstruction has recently been detected also in the Co/Ge(111) system [11,12]. The reconstruction appears in the STM images as an ordered array of clusters. Two types of clusters are present, some of them look dark, the other bright. Structural and electronic properties of the Co/Si(111) $\sqrt{13} \times \sqrt{13}$–$R$ 13.9° reconstruction have been recently treated using high-resolution STM observations and density functional theory (DFT) calculations [4,6]. Structural models of the clusters have been proposed as follows. The dark cluster consists of three Co atoms located in the substitutional sites of the Si(111) surface under one-layer triangle of six Si adatoms [4]. The bright cluster has a similar structure but with three additional Si adatoms located on top of the six Si atoms terminating the dark cluster [6]. One can see that according to these models the Co/Si(111) $\sqrt{13} \times \sqrt{13}$–$R$ 13.9° surface has to contain 3/13 (~0.23) ML Co. However, our recent thorough and accurate evaluations have demonstrated that the actual Co coverage in the Co/Si(111) $\sqrt{13} \times \sqrt{13}$–$R$ 13.9° phase is much greater, ~1.4 ML Co. This finding inspired us to reconsider the structural properties of the Co/Si(111) $\sqrt{13} \times \sqrt{13}$–$R$ 13.9° reconstruction.

In this paper, we report on the results of our work devoted to the evaluation of the Co/Si(111) $\sqrt{13} \times \sqrt{13}$–$R$ 13.9° structure. First, we present our procedure for accurate calibration of the Co evaporator

* Corresponding author at: Institute of Automation and Control Processes, 5 Radio Street, 690041 Vladivostok, Russia.
E-mail address: saranin@iacp.dvo.ru (A.A. Saranin).

http://dx.doi.org/10.1016/j.susc.2014.03.009
0039-6028/© 2014 Elsevier B.V. All rights reserved.

which appears to be crucial for determining the composition of the Co/Si(111) $\sqrt{13} \times \sqrt{13}-R$ 13.9° phase discussed later. We evaluated the composition of both the dark and bright clusters constituting the Co/Si(111) $\sqrt{13} \times \sqrt{13}-R$ 13.9° phase. Then, based on this knowledge we proposed a new structural model of the clusters and test it with DFT calculations, including comparison of simulated STM images with the experimental ones.

2. Experimental and calculation details

Our experiments were performed with an Omicron STM operating in an ultrahigh vacuum (~2.0×10^{-10} Torr). Atomically-clean Si(111) 7×7 surfaces were prepared in situ by flashing to 1280 °C after the samples were first outgassed at 650 °C for several hours. Co was deposited from an electron beam evaporator, vacuum during deposition being better than ~5.0×10^{-10} Torr. For STM observations electrochemically etched tungsten tips cleaned by in situ heating were employed. STM images were acquired at room temperature in the constant-current mode.

To find the energetically favorable structures we have performed ab initio total-energy calculations using the Vienna Ab Initio Simulation Package (VASP) [13–16] based on density functional theory (DFT) [17,18]. The electronic ground state of the system was calculated using the projector-augmented wave (PAW) [19,20] potentials as provided in VASP. The exchange-correlation interaction was described by the Perdew–Wang generalized gradient approximation [21]. The surface was simulated by periodic slab geometry with a unit cell containing five silicon atomic layers and represented here as reconstruction. Hydrogen atoms saturated the dangling bonds of the bottom slab layer. The hydrogen atoms and bottom layer silicon atoms were fixed and the rest of the atoms were free to move. A vacuum gap of approximately 10 Å was incorporated within each periodic unit cell to prevent interaction between adjacent surfaces. The cut-off energy of 300 eV was applied in all calculations presented. Simulated STM images were plotted as the density of states of the surface summed up over the energy interval [22,23] at a constant height of 2.0 Å above the topmost atoms on the surface.

3. Results and discussion

3.1. Calibration of the Co deposition rate

To obtain reliable and accurate calibration of the Co deposition rate we used two complementary techniques. The first one was a standard procedure employing measuring a frequency shift of the crystal quartz monitor. For the set of experiments described in the present paper, the calibration of this type yielded a Co deposition rate of 0.067 ± 0.008 ML/min.

The second technique was based on the knowledge that thin epitaxial Co films grow on the flat Cu(111) layer surface in the layer-by-layer

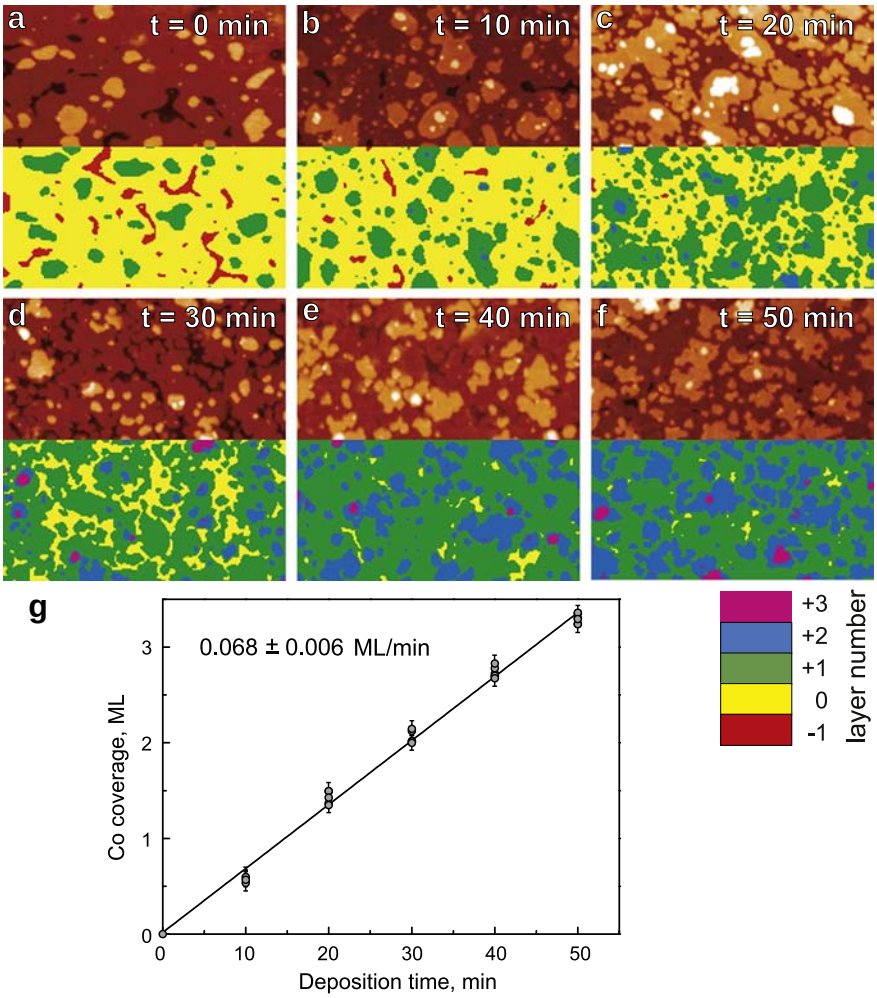

Fig. 1. Calibration of the Co evaporator. 950 × 950 Å^2 filled-state (1.5 V, 1.0 nA) STM images of the Cu/Si(111) surface (a) before and after (b) 10 min., (c) 20 min., (d) 30 min., (e) 40 min., and (f) 50 min. of Co deposition. The lower half of each image indicates the layer numbers according to the palette shown below. (g) Plot of the deposited Co amount versus Co deposition time evaluated from the STM images. Slope of the plot yields Co deposition rate of 0.068 ± 0.006 ML/min.

fashion [24]. In turn, it is known that epitaxial Cu(111) films can be fabricated by depositing Cu onto the Si(111)7 × 7 surface held at RT in which case formation of the intermediate silicide layer of several-monolayers thickness is followed by layer-by-layer growth of the epitaxial Cu(111) film [24–28]. In the present study, the flat Cu(111) surface was prepared by depositing ~20 ML of Cu. Then, cobalt was deposited by small portions keeping the sample also at RT. Morphology of the original epi-Cu/Si(111) surface and that after each Co deposition was monitored with STM.

As illustrated in Fig. 1a, the original epi-Cu/Si(111) surface consists of terraces ("0 level"), flat islands of one-atomic-layer height ("+1 level") and one-atomic-layer deep holes ("−1 level"). To visualize the layer pattern, each layer is indicated in the lower halves of STM images in Fig. 1 by a particular color according to the palette shown below (i.e., red for the "−1 level", yellow for the "0 level", green for the "+1 level", blue for the "+2 level", and violet for the "+3 level"). Growth of Co epi-layer starts mainly from the step edges presented on the original surface, though nucleation of the new islands also takes place. STM contrast of the Co layer appears to be very similar to that of Cu. Thus, Co deposition results apparently in filling the holes, expanding the islands and nucleating the next-level islands atop the existing islands. Measuring the change in the surface area occupied by each level after deposition of Co, one obtains a direct evaluation of the deposited Co amount. Results of such an evaluation are summarized in

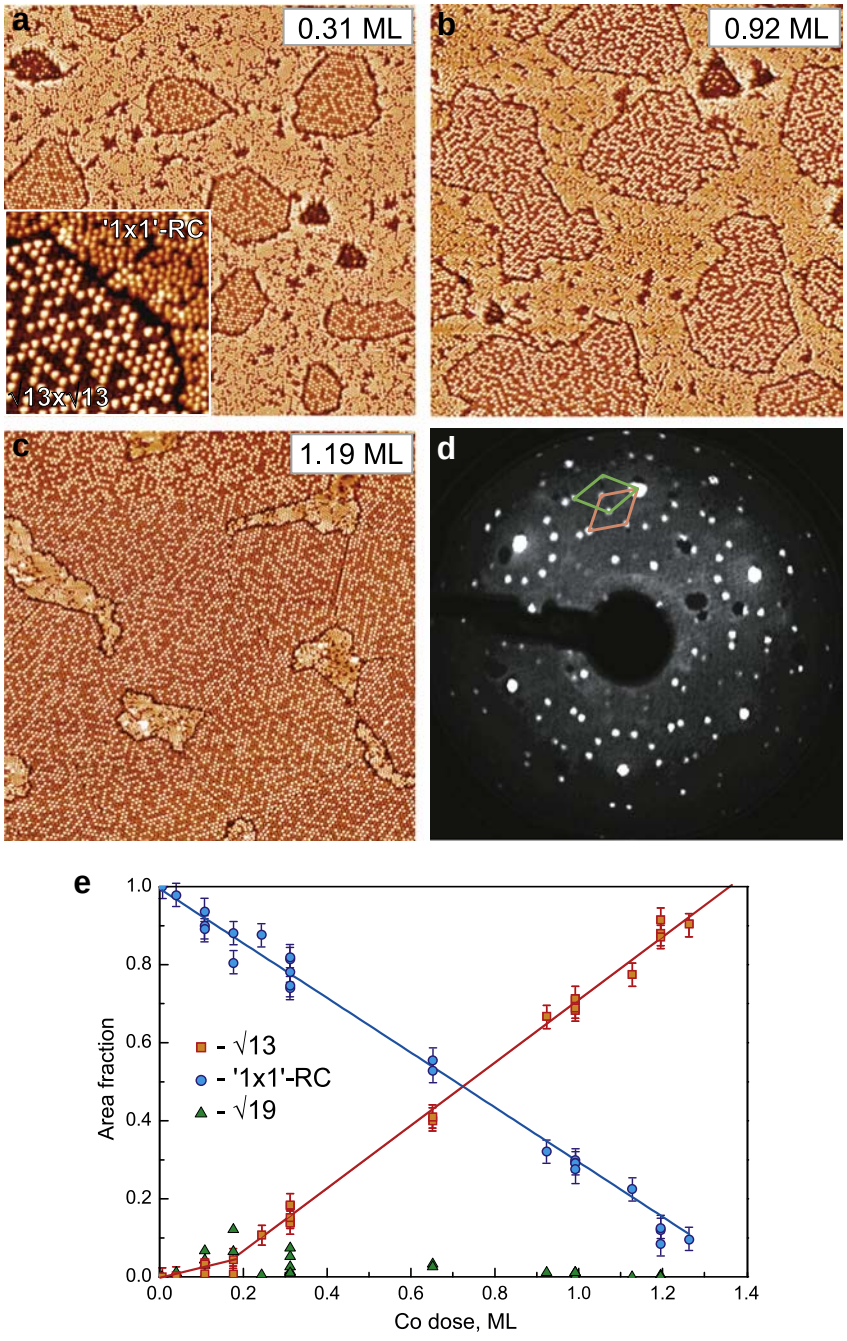

Fig. 2. Formation of the Co/Si(111) $\sqrt{13} \times \sqrt{13}$–$R$ 13.9° surface by depositing Co onto the "1 × 1"-RC surface held at ~550 °C. 1500 × 1500 Å^2 filled-state (−2.0 V, 1.0 nA) STM images of the surface after deposition of (a) 0.31, (b) 0.92, and (c) 1.19 ML. Inset in (a) show the surface structure at a greater magnification (scale: 300 × 300 Å^2) to visualize the difference in the STM contrast of the $\sqrt{13} \times \sqrt{13}$ and "1 × 1"-RC domains. (d) Sharp $\sqrt{13} \times \sqrt{13}$ LEED pattern (E_p = 55 eV) from the surface shown in (c). The $\sqrt{13} \times \sqrt{13}$ reciprocal lattice unit cells for two rotational domains are indicated. (e) Evolution of the area fraction occupied by "1 × 1"-RC (blue circles, blue line), $\sqrt{13} \times \sqrt{13}$ (red squares, red line), and minor $\sqrt{19} \times \sqrt{19}$ (green triangles, green line) in the course of Co deposition. (For interpretation of the references to color in this figure legend, the reader is referred to the web version of this article.)

the graph in Fig. 1. The determined Co deposition rate appears to be 0.029 ± 0.002 ML/min. in the units of Co(111) monolayers, 1.83 × 10^{15} cm^{-2}. For Si(111) monolayer units, 7.8 × 10^{14} cm^{-2}, this corresponds to 0.068 ± 0.006 ML/min. in excellent agreement with the calibration obtained with a quartz monitor.

3.2. Composition of the Co/Si(111) $\sqrt{13} \times \sqrt{13}-R$ 13.9°

To prepare the homogeneous Co/Si(111) $\sqrt{13} \times \sqrt{13}-R$13.9° surface, a two-step procedure was employed. At the first step, the "1 × 1"-RC surface was fabricated by adsorption of ~0.05–0.10 ML Co onto Si(111)7 × 7 surface held at 810–825 °C [29,30] followed by rapid cooling. The "1 × 1"-RC surface appears to be a promising template for growing well-ordered Co/Si(111) reconstructions. In particular, we have recently shown that deposition of Co onto this surface with gradual decrease of temperature from 800 to 700 °C produces the well-ordered Co/Si(111) $\sqrt{7} \times \sqrt{7}-R$ 19.1° surface with domain size as large as ~1000 Å [31]. In the present study, Co was deposited onto the "1 × 1"-RC surface held at lower temperature of ~550 °C that resulted in developing Co/Si(111) $\sqrt{13} \times \sqrt{13}-R$ 13.9° surface. One can see in Fig. 2 that area fraction occupied by the $\sqrt{13} \times \sqrt{13}-R$ 13.9° phase grows linearly with deposited Co dose and the phase occupies almost the entire surface after deposition of about 1.3 ML Co. Taking into account that original "1 × 1"-RC surface contains 0.05 to 0.10 ML Co, one obtains an estimation that the $\sqrt{13} \times \sqrt{13}-R$ 13.9° surface adopts ~1.4 ML Co.

One can argue that for the evaluation it was assumed that no Co atoms were lost from the surface during the $\sqrt{13} \times \sqrt{13}-R$ 13.9° phase formation. Though the formation temperature of 550 °C indeed seems to be too low to induce noticeable Co desorption, we conducted two experiments to prove this assumption directly. In the first experiment, the same Co amount of ~1.3 ML was deposited onto the "1 × 1"-RC surface at RT and annealed at 680 °C. In the second experiment, the Co/Si(111) $\sqrt{13} \times \sqrt{13}-R$ 13.9° surface formed according to the technique described above was also annealed at 680 °C. The resultant surfaces in both cases represent arrays of $CoSi_2$ islands in agreement with the published data [32]. As an example, Fig. 3a shows the surface obtained in the first experiment. From the measured heights (Fig. 3b) and areas of the islands and taking into account that they have CaF_2-type structure, we evaluated the amount of Co present at the surface. It appeared to be 1.37 ± 0.15 ML Co in the first experiment and 1.29 ± 0.15 ML Co in the second one. Both values are consistent with evaluation for the $\sqrt{13} \times \sqrt{13}-R$ 13.9° reconstruction proving that 1.4 ± 0.2 ML is its actual plausible Co coverage.

Another important characteristic of any reconstruction on silicon besides adsorbate coverage is the coverage of Si atoms incorporated in the reconstruction. When transition between two reconstructions having different Si-atom coverage takes place at relatively low temperature (when long-range Si migration is limited), domains of the new reconstruction typically develops in two levels, namely as "hole-island" pairs. Occurring of the $\sqrt{13} \times \sqrt{13}-R$ 13.9° reconstruction almost in a single level upon transformation from the "1 × 1"-RC phase (Fig. 2) indicates an absence of considerable Si mass transport, hence the $\sqrt{13} \times \sqrt{13}-R$ 13.9° and "1 × 1"-RC surfaces have plausibly close Si-atom coverages. Note that "1 × 1"-RC surface is actually a random uncompleted array of ring clusters and its composition is not well-defined. Thus, one can obtain only an estimate that its Si-atom coverage is in between 102/49–2.08 ML of the original Si(111)7 × 7 surface and 19/7–2.71 ML of the completed RC array in the $\sqrt{7} \times \sqrt{7}-R$ 19.1° phase. Therefore, this interval can be considered as an estimate for the Si-atom coverage of the $\sqrt{13} \times \sqrt{13}-R$ 13.9° phase.

Occurrence of the clusters of two types, dark and bright, at the $\sqrt{13} \times \sqrt{13}-R$ 13.9° surface is also related to the surface Si contents. It was suggested [4,6] that the bright cluster differs from the dark cluster by three additional Si atoms adsorbed on its top. To check this assumption, we conducted the experiment in which Si was deposited onto the $\sqrt{13} \times \sqrt{13}-R$ 13.9° held at RT and the density of bright clusters was measured as a function of Si dose. The representative STM images at various stages of Si deposition and the plot of bright cluster fraction versus Si dose are shown in Fig. 4. At the original $\sqrt{13} \times \sqrt{13}-R$ 13.9° surface, the bright clusters comprise about 60% in agreement with the reported data [4,6] and their density grows linearly with deposited Si dose until they constitute ~93% and other features start to grow in between the clusters. The slope of the plot apparently corresponds to the case when each new bright cluster adopts three additional Si atoms. In other words, adding three Si atoms to the dark cluster converts it to the bright cluster.

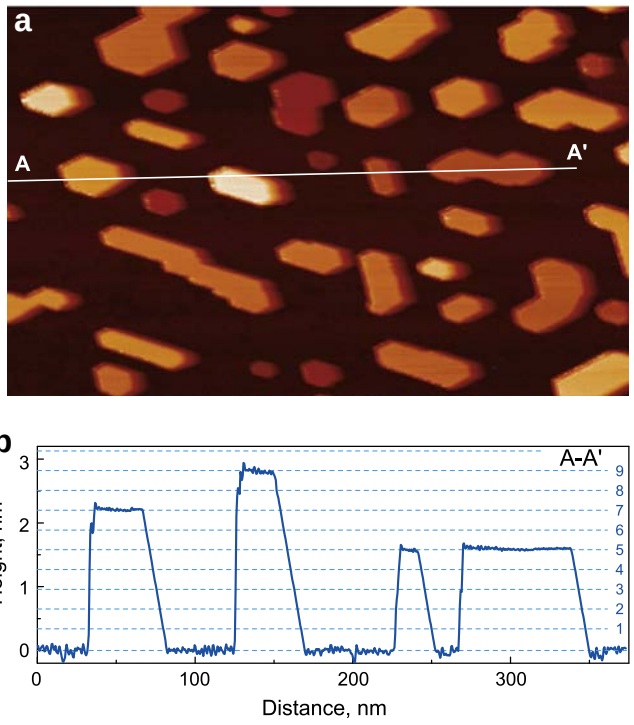

Fig. 3. (a) 4000 × 2500 $Å^2$ filled-state (−2.3 V, 1.2 nA) STM image from the surface formed by RT deposition of ~1.3 ML of Co followed by annealing at 680 °C. The surface contains $CoSi_2$ islands with flat top. (b) Line profile along the line A–A′ in (a) showing the island heights. In particular, the shown islands contain five, seven and nine $CoSi_2$ monolayers (shown at the right axis scale).

Results of the composition evaluation can be summarized as follows. The Co/Si(111) $\sqrt{13} \times \sqrt{13}-R$ 13.9° surface phase incorporates 1.4 ± 0.2 ML Co. The Si-atom coverage in it belongs to the interval from ~2.1 to ~2.7 ML. Compared to the dark clusters, each bright cluster contains three additional Si atoms.

3.3. Structural models of the Co/Si(111) $\sqrt{13} \times \sqrt{13}-R$ 13.9°

The previous structural model [4,6] (for the dark cluster) presents essentially a cluster where three Co atoms are located in the substitutional sites of the Si(111) surface under one-layer triangle of six Si adatoms. The DFT calculations demonstrated that this configuration is stable and its simulated STM images are in a reasonable agreement with the experimental images [4,6]. However, the Co amount adopted by the model structure (3/13–0.23 ML) is by ~1 ML less than that determined in the present experiments. It is worth to remark, however, that the found value does not contradict greatly the experimental data of Refs. [4,6]. Namely, it is reported in Ref. [4] that after deposition of 0.2 ML Co and subsequent annealing at 800 K the surface is mainly covered by $\sqrt{7} \times \sqrt{7}-R$ 19.1° domains while $\sqrt{13} \times \sqrt{13}-R$ 13.9° zones occupy about 7% of the total surface area. Taking into account that $\sqrt{7} \times \sqrt{7}-R$ 19.1° phase is known to incorporate 1/7

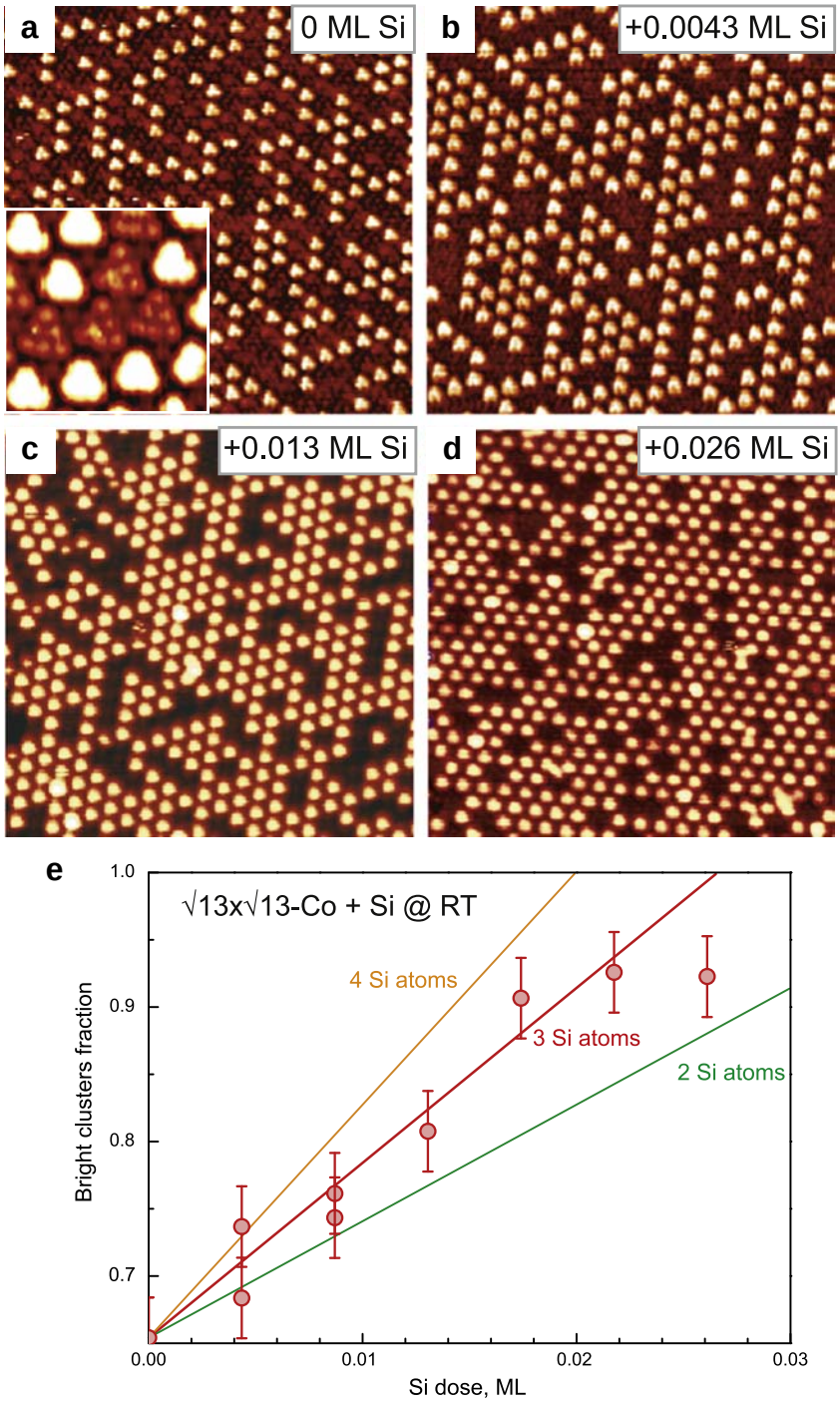

Fig. 4. Formation of additional bright clusters in the course of Si deposition onto Si(111) $\sqrt{13} \times \sqrt{13}$–$R$ 13.9°-Co deposition held at RT. 300 × 300 Å^2 filled-state (−2.3 V, 1/0 nA) STM images showing the surface (a) before and after deposition of (b) 0.04, (c) 0.013 and (d) 0.026 ML Si. Inset in (a) shows STM appearance of the bright and dark clusters at a greater magnification. (e) Dependence of the bright cluster fraction versus deposited Si dose. The linear plots show the calculated dependencies for the cases when each bright cluster adopts two Si atoms (green line), three Si atoms (red line) and four Si atoms (yellow line). (For interpretation of the references to color in this figure legend, the reader is referred to the web version of this article.)

(~0.14) ML Co, one obtains a rough estimate of ~1.0 ML Co coverage for $\sqrt{13} \times \sqrt{13}$– R 13.9° reconstruction.].

The Co coverage determined for the Co/Si(111) $\sqrt{13} \times \sqrt{13}$–$R$ 13.9° phase demands reconsideration of its structural model. To reconcile the promising cluster model with result of Co coverage determination, we have suggested that the Co–Si cluster resides not at the original Si(111) surface (as suggested previously) [4,6], but rather on the silicide Si–Co–Si triple layer on Si(111).

Following this assumption, we have tested about forty various structural models (with different types of silicide interface, with completed and uncompleted Si–Co–Si triple layers, with clusters of different composition, etc.) of which the two (for the dark cluster) having the lowest formation energies are shown in Fig. 5a and b. Both models have a similar composition, namely each one adopts 16/13–1.23 ML Co and 33/13–2.54 ML Si in a general agreement with the results of experimental evaluation of the Co/Si(111) $\sqrt{13} \times \sqrt{13}$–$R$ 13.9°

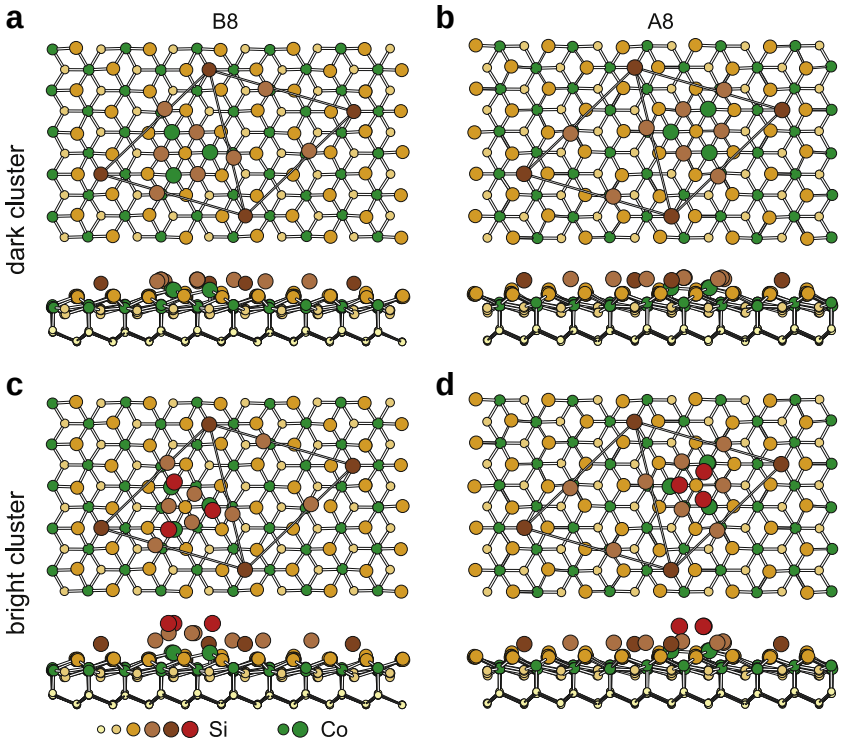

Fig. 5. Structural models of the Si(111) $\sqrt{13} \times \sqrt{13}$–$R$ 13.9°-Co proposed for (a, b) dark and (c, d) bright clusters. The models in (a, c) and (b, d) adopt Si(111)-silicide interfaces of B8- and A8-types, respectively. Co atoms are shown by green circles, Si atoms of different layers are shown by circles of different colors from yellow to red and of different sizes which increase from the bottom to the top. (For interpretation of the references to color in this figure legend, the reader is referred to the web version of this article.)

composition. As a basic element, both models adopt the cluster similar to that proposed in Refs. [4,6]. According to the models, the top Si layer contains seven Si atoms per $\sqrt{13} \times \sqrt{13}$ unit cell of which six Si atoms are incorporated into the cluster and the seventh Si atom occupies a threefold-coordinated adatom position (in the corner of the outlined unit cell in Fig. 5). Both models contain a similar silicide Si–Co–Si triple layer with eightfold coordination of Co atoms and differ only by stacking of the silicide layer to the Si(111) substrate, either with silicide unit cell oriented like that of Si or rotated by 180°. Following the accepted notation [33], they are defined as A8 and B8 interfaces, respectively. Hence, the proposed models will be referred as A8 model (Fig. 5b) and B8 model (Fig. 5a), respectively. The B8 model represents the lowest-energy configuration, but the A8 model is less stable by only 0.3 eV per $\sqrt{13} \times \sqrt{13}$ unit cell and cannot be conclusively ruled out. Adding three extra Si atoms produces the bright clusters which calculated structures are shown in Fig. 5c and d for the A8 and B8 models, respectively. Note that placing Si atom above the triangle made of the lower three Si atoms (especially, as in case of the B8 model) resembles atomic arrangement of Si magic clusters observed on Si(111)7 × 7 surface [34].

Fig. 6 shows the simulated STM images for the two A8 and B8 models (for dark and bright clusters) in comparison with the experimental STM images. Since the arrangement of the top atomic layers in the A8 and B8 models is very similar (especially for the dark clusters), their simulated STM images are also similar. Both models demonstrate a fair resemblance between simulated and experimental STM images except for a small difference. Namely, the features associated with Si adatoms in the corners of the unit cell are absent in the simulated empty-state STM images. This is thought to be a natural sequence of the large height difference between the top Si atoms in the Co–Si cluster and the Si adatoms (~1.6–1.9 Å depending on the model). Note that a simulated STM image presents a constant-height cross section of the integrated density of states, hence the lower the height of a particular atomic feature the smaller is its contribution to the image. In contrast, experimental STM images were acquired in a constant-current mode which allows probing features located at the different heights.

As a final remark, we would like to note that the $\sqrt{13} \times \sqrt{13}$–$R$ 13.9°-Co structure might not be unique. First, we could remind occurrence of the so-called β–$\sqrt{13}$–R 13.9°-Co phase reported by Cui et al. [2] which is free of bright clusters and has STM appearance different from that of the $\sqrt{13} \times \sqrt{13}$–$R$ 13.9°-Co reconstruction discussed in the present paper. However, it should be remarked that this β–$\sqrt{13}$–R 13.9°-Co phase has not been observed in other studies, including the present one. Another example is presented by the $\sqrt{13} \times \sqrt{13}$–$R$ 13.9°-Co phase which has recently been found in Co/Ge(111) system [11,12]. This phase is also free of bright clusters and has a specific STM appearance. Authors of the two papers proposed two alternative models for the Ge(111) $\sqrt{13} \times \sqrt{13}$–$R$ 13.9°-Co structure. While Mocking et al. [11] suggested the model similar to that reported by Wetzel with coworkers [4,6], Muzychenko et al. [12] proposed the original model with six Co atoms per $\sqrt{13} \times \sqrt{13}$ unit cell (hence, with ~0.46 ML Co). Unfortunately, accurate data on the composition of the Ge(111) $\sqrt{13} \times \sqrt{13}$–$R$ 13.9°-Co phase is lacking. But reported experimental observation [12] after depositing about 0.25 ML Co, the $\sqrt{13}$–R 13.9°-Co domains occupy 23% ± 7% of the surface area (the left surface being free of Co) and might indicate that actual Co coverage in that Ge(111) $\sqrt{13} \times \sqrt{13}$–$R$ 13.9°-Co phase is greater than ~0.23 or ~0.46 ML suggested by the models. Note that placing the cluster proposed by Muzychenko et al. [12] onto the Si–Co–Si triple layer produces a structure with ~1.46 ML Co and this Co coverage is also consistent with experimental value determined in the present study. However, our DFT calculations demonstrated that the structures of this type are less stable than the models shown in Fig. 5. Thus, we can state that additional experimental and theoretical efforts are required to solve all puzzles of the $\sqrt{13} \times \sqrt{13}$–$R$ 13.9°-Co reconstructions on Si(111) and Ge(111) surfaces.

4. Conclusions

In conclusion, the Si(111) $\sqrt{13} \times \sqrt{13}$–$R$ 13.9°-Co surface shows up in the STM images as an ordered array of cluster-like structures,

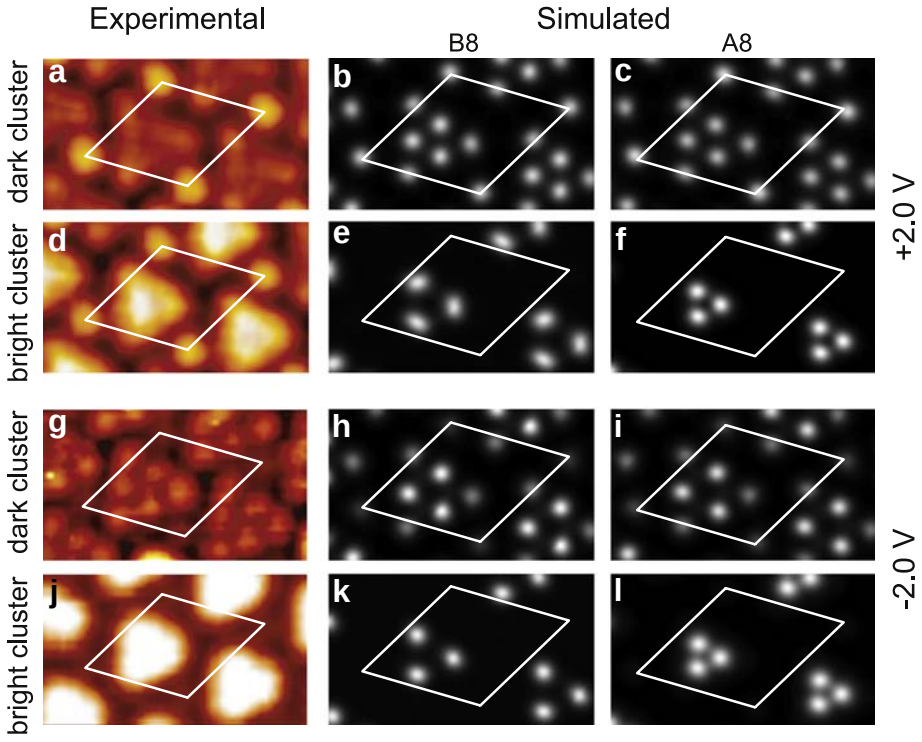

Fig. 6. Experimental STM images of the Si(111) $\sqrt{13} \times \sqrt{13}$–$R$ 13.9°-Co surface (a, d, g, j) and STM images simulated for the B8 model (b, e, h, k) and the A8 model (c, f, i, l). (a to f) are for the empty-state STM images with sample bias of +2.0 V, (g to l) are for the filled-state STM images with sample bias of −2.0 V. (a, b, c, g, h, i) represent the images of the dark cluster, (d, e, f, j, k, l) represent those of the bright cluster which adopts three additional Si atoms.

including two types of clusters looking dark and bright. Upon thorough experimental evaluation of the surface composition, we have established that the surface incorporates 1.4 ± 0.2 ML of Co and adding three Si atoms to the dark cluster converts it to the bright cluster. The recently proposed structural models of the dark [4] and bright [6] clusters suggest that each cluster contains three Co atoms, hence the corresponding Co coverage is 3/13–0.23 ML which is by ~1 ML less than that determined in the present experiments. To resolve this inconsistency we have suggested that the clusters reside not at the original Si(111) surface (as suggested previously), but on the silicide Si–Co–Si triple layer on Si(111) substrate. About forty various models of this type have been tested using DFT calculations and the two models with A8 and B8 silicide/Si(111) interfaces have been found to represent the most stable configurations.

Acknowledgments

Part of this work was supported by the Russian Foundation for Basic Research (Grant nos. 12-02-00416 and 13-02-00837), and the Ministry of Education and Science of the Russian Federation (Grant no. NSh-167.2014.2).

References

[1] M. Löffler, J. Cordón, M. Weinelt, J.E. Ortega, T. Fauster, Appl. Phys. A 81 (2005) 1651.
[2] Y.T. Cui, T. Xie, M. Ye, A. Kimura, S. Qiao, H. Namatame, M. Taniguchi, Appl. Surf. Sci. 254 (2008) 7684.
[3] F. Dulot, M.C. Hanf, P. Wetzel, Surf. Sci. 602 (2008) 1447.
[4] L. Chaput, F. Dulot, M.C. Hanf, P. Wetzel, Surf. Sci. 604 (2010) 513.
[5] M. Odagiri, I. Mochizuki, Y. Shigeta, A. Tosaka, Appl. Phys. Lett. 97 (2010) 151911.
[6] Z. Yuan, P. Sonnet, M.C. Hanf, R. Stephan, F. Dulot, P. Wetzel, Surf. Sci. 607 (2013) 111.
[7] P.A. Bennett, M. Copel, D. Cahill, J. Falta, R.M. Tromp, Phys. Rev. Lett. 69 (1992) 1224.
[8] M.H. Tsai, J.D. Dow, P.A. Bennett, D.G. Cahill, Phys. Rev. B 48 (1993) 2486.
[9] S.A. Parikh, M.Y. Lee, P.A. Bennett, Surf. Sci. 356 (1996) 53.
[10] A.E. Dolbak, B.Z. Olshanetsky, S.A. Teys, Surf. Sci. 373 (1997) 43.
[11] T.F. Mocking, B. Poelsema, H.J.W. Zandvliet, Surf. Sci. 610 (2013) 59.
[12] D.A. Muzychenko, K. Schouteden, Haesendonck C. Van, Phys. Rev. B 88 (2013) 195436.
[13] G. Kresse, J. Hafner, Phys. Rev. B 47 (1993) 558.
[14] G. Kresse, J. Hafner, Phys. Rev. B B49 (1994) 14251.
[15] G. Kresse, J. Furthmüller, Phys. Rev. B 54 (1996) 11169.
[16] G. Kresse, J. Furthmüller, Comput. Mater. Sci. 6 (1996) 15.
[17] P. Hohenberg, W. Kohn, Phys. Rev. 136 (1964) B864.
[18] W. Kohn, L.J. Sham, Phys. Rev. 140 (1965) A1133.
[19] P.E. Blöchl, Phys. Rev. B 50 (1994) 17953.
[20] G. Kresse, D. Joubert, Phys. Rev. B 59 (1999) 1758.
[21] J.P. Perdew, Y. Wang, Phys. Rev. B 45 (1992) 13244.
[22] J. Tersoff, D.R. Hamann, Phys. Rev. B 31 (1985) 805.
[23] R.M. Feenstra, Surf. Sci. 299 (300) (1994) 965.
[24] Yu.P. Ivanov, A.I. Ilin, A.V. Davydenko, A.V. Zotov, J. Appl. Phys. 110 (2011) 083505.
[25] T.I.M. Bootsma, T. Hibma, Surf. Sci. 331 (333) (1995) 636.
[26] Z.H. Zhang, S. Hasegawa, S. Ino, Surf. Sci. 415 (1998) 363.
[27] K. Pedersen, T.B. Kristensen, T.G. Pederser, P. Morgen, Z. Li, S.V. Hoffman, Phys. Rev. B 66 (2002) 153406.
[28] A.V. Zotov, D.V. Gruznev, O.A. Utas, V.G. Kotlyar, A.A. Saranin, Surf. Sci. 602 (2008) 391.
[29] R.J. Phaneuf, Y. Hong, S. Horch, P.A. Bennet, Phys. Rev. Lett. 78 (1997) 4605.
[30] R.J. Phaneuf, P.A. Bennet, M. Marsi, S. Günther, L. Gregoratti, L. Casalis, M. Kiskinova, Surf. Sci. 431 (1999) 232.
[31] D.A. Olyanich, T.V. Utas, V.G. Kotlyar, A.V. Zotov, A.A. Saranin, L.N. Romashev, N.I. Solin, V.V. Ustinov, Appl. Surf. Sci. 292 (2014) 954.
[32] M.A.K. Zilani, L. Liu, H. Xu, Y.P. Feng, X.S. Wang, A.T.S. Wee, J. Phys. Condens. Matter 18 (2006) 6987.
[33] S. Walter, F. Blobner, M. Krause, S. Müller, K. Heinz, U. Starke, J. Phys. Condens. Matter 15 (2003) 5207.
[34] W. Ong, E.S. Tok, H. Johll, H.C. Kang, Phys. Rev. B 79 (2009) 235439.